Boletim da Sociedade Astronômica Brasileira, **37**, no. 1, 81-84

Physical-chemical characterization of the GJ 3470 b exoplanetary system

Cinthya Cerqueira[1], Diogo Souto[1], Natasha E. Batalha[2], Anderson Silva Andrade[1], & Eder Martioli[3]

[1] Departamento de Física, Universidade Federal de Sergipe, Av. Marcelo Deda Chagas, s/n, 49107-230, São Cristóvão, SE, Brazil
[2] NASA Ames Research Center, Moffett Field, CA 94035, USA
[3] Laboratório Nacional de Astrofísica, Rua Estados Unidos 154, 37504-364, Itajubá, MG, Brazil

Abstract. The characterization of planetary systems is essential for understanding their formation, evolution, and atmospheric composition. This work combines high-resolution spectroscopic analysis of the host star with low-resolution data from the exoplanet's atmosphere. The system studied is GJ 3470, comprising an M-dwarf star and the warm Neptune exoplanet GJ 3470 b. The present analysis focuses on stellar spectra obtained with the SPIRou instrument, which provides high-resolution near-infrared coverage (R ~70,000). The stellar spectra were processed by normalizing them, applying radial-velocity corrections via cross-correlation, and combining the individual observations. The high signal-to-noise spectra obtained enable precise determination of fundamental stellar parameters, including effective temperature, surface gravity, metallicity, and the chemical abundances of C, O, Na, Mg, Al, Si, K, Ca, Ti, V, Cr, Mn, Fe, and Ni. Based on the physical and chemical properties determined for the host star, we performed a spectroscopic characterization of the atmosphere of the exoplanet GJ 3470 b using JWST observations with the NIRCam instrument and the PICASO radiative-transfer and modeling code, combined with Bayesian inference via `MCMC` sampling. Our results indicate that the exoplanet's atmosphere is enriched in SO_2, CO_2, and H_2O.

Resumo. A caracterização de sistemas planetários é fundamental para compreender sua formação, evolução e composição atmosférica. Este trabalho integra a análise espectroscópica de alta resolução da estrela hospedeira com dados de baixa resolução provenientes da atmosfera do exoplaneta. O sistema estudado é GJ 3470, composto por uma anã M e pelo exoplaneta do tipo Netuno quente GJ 3470 b. A análise atual concentra-se em espectros estelares obtidos com o instrumento SPIRou (CFHT), que fornece cobertura no infravermelho em alta resolução (R ~ 70,000). Os espectros foram processados com etapas de normalização, correção de velocidade radial por correlação cruzada e combinação das diversas observações. Como resultado parcial, foi obtido um espectro combinado, permitindo a determinação precisa de parâmetros fundamentais da estrela hospedeira, como temperatura efetiva, gravidade superficial, metalicidade e abundâncias químicas de C, O, Na, Mg, Al, Si, K, Ca, Ti, V, Cr, Mn e Fe. Com base nos parâmetros físicos e químicos da estrela, realizamos a caracterização espectroscópica da atmosfera do exoplaneta GJ 3470 b utilizando observações do JWST com o instrumento NIRCam, e o código PICASO para modelagem e transferência radiativa, associado a métodos Bayesianos baseados em amostragem `MCMC`. Nossos resultados preliminares indicam que a atmosfera do exoplaneta apresenta composição enriquecida em SO_2, CO_2 e H_2O.

Keywords. Planets and satellites: individual: GJ 3470 b – Planets and satellites: atmospheres – Stars: individual: GJ 3470 – Stars: fundamental parameters

1. Introduction

M dwarf stars are currently prime targets in the search for small exoplanets. Owing to their low masses and radii, orbiting planets produce stronger observational signatures, thereby enhancing detectability and enabling more precise spectroscopic characterization—particularly for close-in planets within the habitable zone or those exhibiting deep transits. Moreover, M dwarfs are the most common stellar type in the Milky Way, representing more than 70% of the stellar population (Henry et al. 2006). Their long main-sequence lifetimes and slow evolutionary timescales also make them valuable probes of the interstellar medium's chemical composition at the time of their formation.

Transit surveys such as Kepler (Borucki et al. 2010) and TESS (Ricker et al. 2010) have shown that Neptune and sub-Neptune like exoplanets, typically defined by having a radii between 1 and 4 $R_\oplus$ and orbital periods shorter than 100 days, is absent from the Solar System yet appears to be one of the most common populations in the Milky Way (Batalha et al. 2013; Petigura et al. 2013; Bean et al. 2021). The advent of the James Webb Space Telescope (JWST) has further intensified interest in these worlds by enabling high-precision spectroscopic observations well suited to detailed atmospheric characterization.

Motivated by this broader context, this work focuses on the GJ 3470 system, which comprises an M dwarf host star and the sub-Neptune GJ 3470 b. We aim to determine the effective temperature ($T_{\rm eff}$) and metallicity ([Fe/H] and with these refined stellar parameters in hand, we then characterize the atmosphere of GJ 3470 b through photochemical and radiative transfer modeling, followed by a comparison with the planet's transmission spectrum as observed by JWST.

2. Stellar atmospheric parameters and abundances

To characterize the host star GJ 3470, we used high-resolution near-infrared spectra obtained with SPIRou. The dataset comprises 107 observations spanning the spectral range from 0.95 to 2.35 μm. We limited our wavelength between 1.5-1.7 μm. This is the same region covered by the APOGEE spectra from the Sloan Digital Sky Survey (SDSS)-IV (Blanton et al. 2017). We adopt the same stellar parameters and individual abundance analysis, which are well established using APOGEE spectra in the literature (Melo et al. (2024), Wanderley et al. (2025)).

We used the SPIRou spectra already corrected for telluric absorption by the `APERO` Data Reduction Software pipeline (Cook et al. 2022). Each spectrum was initially normalized by fitting and removing the continuum using the `Spectrum1D` class from the `specutils` library. The continuum was estimated with the `fit_generic_continuum` function, and the flux was divided by the resulting model. A subsequent rescaling, based on the

median of the highest flux values in each segment, was applied to ensure consistency across spectral orders. Following these steps, the normalized segments were concatenated and reordered to produce a complete spectrum for each observation.

To align the spectra, we computed the relative wavelength shift $\Delta\lambda$ for each observation by minimizing the point-by-point χ^2 with respect to a reference spectrum, applying the resulting shift exclusively to the wavelength array. Once all spectra were aligned, we constructed a combined spectrum using the reference spectrum's wavelength grid. For each wavelength point, we selected the corresponding flux values from the 107 observations within a tolerance of 0.02,Å and applied a 3σ sigma-clipping procedure to remove outliers. The final flux for each wavelength was then computed as the mean of the remaining values. The resulting combined spectrum, as shown in the black solid line in Figure 1, was subsequently used in the spectroscopic analysis.

The stellar parameters were determined using the `BACCHUS` code (Masseron et al. 2016), which employs LTE atmospheric modeling, MARCS model atmospheres (Gustafsson et al. 2008), and spectral synthesis performed with `Turbospectrum` (Plez 2012). For comparison, we repeated the same analysis using the APOGEE spectrum of GJ 3470. Following the methodology of Souto et al. (2020), we derived the stellar effective temperature and metallicity. For $T_{\rm eff}$, we use two sets of indicators: OH and H2O molecular lines ($T_{\rm eff}$–A(O)) and Fe I plus FeH lines ($T_{\rm eff}$–A(Fe)). As noted by Souto et al. (2020), Fe-based diagnostics tend to yield systematically higher temperatures. Using these methods, we obtained $T_{\rm eff} = 3722 \pm 100$ K for the SPIRou spectrum and $T_{\rm eff} = 3678 \pm 100$ K for the APOGEE spectrum. For metallicity, we derived [Fe/H] $= 0.14 \pm 0.14$ dex from the combined SPIRou spectrum and [Fe/H] $= 0.18 \pm 0.14$ dex from the APOGEE spectrum.

Using bolometric corrections from Mann et al. (2015) and following the method of Souto et al. (2020), we calculated the star's luminosity, radius, and mass, allowing us to derive orbital and physical parameters for GJ 3470 b. The derived stellar and exoplanet parameters are shown in Table 1.

3. Modeling GJ 3470 b atmosphere with PICASO

Using the stellar and orbital parameters determined for the GJ 3470 system, including the host star's radius and temperature, the planet's semi-major axis, and its equilibrium temperature, we modeled the atmospheric structure of GJ 3470 b with the `PICASO` code (Batalha et al. 2019; Mukherjee et al. 2023). `PICASO` couples a radiative-transfer module with a photochemistry solver, enabling the computation of temperature–pressure profiles and chemical abundances under both equilibrium and disequilibrium conditions.

Figure 2 presents the temperature–pressure profile across the atmosphere of GJ 3470 b. At low pressures (high altitudes), the temperature is relatively low and increases gradually with rising pressure, reaching values above 4000 K in the deepest atmospheric layers. This characteristic structure reflects stellar heating in the upper atmosphere and the increase in temperature due to compressional heating in the deeper regions.

Figure 3 shows the chemical abundances of H_2O, CH_4, CO, CO_2, SO_2, and NH_3 as a function of pressure. The high abundances of heavy species such as H_2O, CO, and CO_2 are indicative of a metal-rich atmosphere, as enhanced concentrations of these molecules are directly associated with elevated heavy element–to–hydrogen ratios.

For GJ 3470 b, whose equilibrium temperature is relatively low ($T_{\rm eq} \approx 597$ K), the significant production of SO_2 would not be expected from thermochemical processes alone. Instead, its presence is linked to photochemistry: the high abundance of H_2O enhances photolysis in the upper atmosphere, producing OH radicals that oxidize H_2S into SO_2. The resulting SO_2 therefore serves as a direct tracer of active photochemical pathways and indicates that the atmosphere is not in chemical equilibrium.

Another important aspect is the role of vertical transport. Because GJ 3470 b exhibits efficient vertical mixing, chemical quenching occurs at relatively deep pressures: species are carried upward to lower-pressure regions before they can reach thermodynamic equilibrium. This behavior explains why CO remains the dominant carbon-bearing molecule even at temperatures where methane would be favored under equilibrium conditions. The persistence of CO at high abundances, together with the photochemical production of SO_2, reinforces the interpretation of an atmosphere that strongly departs from chemical equilibrium and experiences vigorous vertical mixing.

To fit the JWST/NIRSpec transmission spectrum of GJ 3470 b (Beatty et al. 2024), we used a grid of atmospheric models (RCTE_cld; Mukherjee et al. 2023; Rooney et al. 2022; Batalha et al. 2019) generated with the `PICASO` code. The grid spans six physical parameters: internal temperature, metallicity, C/O ratio, heat-redistribution efficiency, cloud-settling parameter, and vertical mixing coefficient. Each theoretical spectrum was resampled onto the observational wavelength grid and adjusted by a constant offset in transit depth to ensure proper alignment between the models and the data.

Bayesian inference was carried out using the `emcee` sampler (Foreman-Mackey et al. 2013), which implements the Markov Chain Monte Carlo (MCMC) algorithm. For each parameter set explored, we identified the nearest models within the grid and performed multidimensional interpolation to estimate the corresponding spectrum. Uniform priors were adopted, and the likelihood was defined by a Gaussian χ^2 function comparing the observed transmission spectrum with the interpolated model.

The posterior distributions (Figure 4) indicate an internal temperature of roughly 200 K, a high metallicity on the order of 100 times the solar value, and a C/O ratio near the upper limit of the explored range (approximately 0.92). The narrow posterior on the C/O ratio suggests a strong preference for carbon-rich models; however, this behavior may also reflect limitations of the model grid, as interpolation can force solutions toward the edges when intermediate models fail to reproduce certain spectral features.

The inferred heat-redistribution parameter (heat$_{\rm r}$edis ≈ 0.4) implies partial redistribution of the incident stellar energy. In the PICASO framework, values near 0.5 correspond to full redistribution between the day and night hemispheres, whereas values near 1.0 indicate re-radiation confined to the dayside. Thus, a value of 0.4 suggests efficient transport of heat to the nightside, though not sufficient to produce full day–night thermal equilibration. The retrieved cloud-settling parameter ($f_{\rm sed} \approx 3$) is consistent with moderately thick clouds. At the same time, the vertical mixing coefficient ($\log K_{zz} \approx 9$) indicates vigorous vertical transport, characteristic of dynamically active atmospheres.

Overall, the results are consistent with trends observed in hot sub-Neptunes, which commonly exhibit metal-rich atmospheres, strong vertical mixing, and cloud layers that partially mute spectral features. These characteristics suggest that GJ 3470 b possesses a metal-enriched, moderately cloudy, and dynamically vigorous atmosphere.

4. Conclusions

In this work, we characterized the GJ 3470 system through a combination of high-resolution stellar spectroscopy obtained

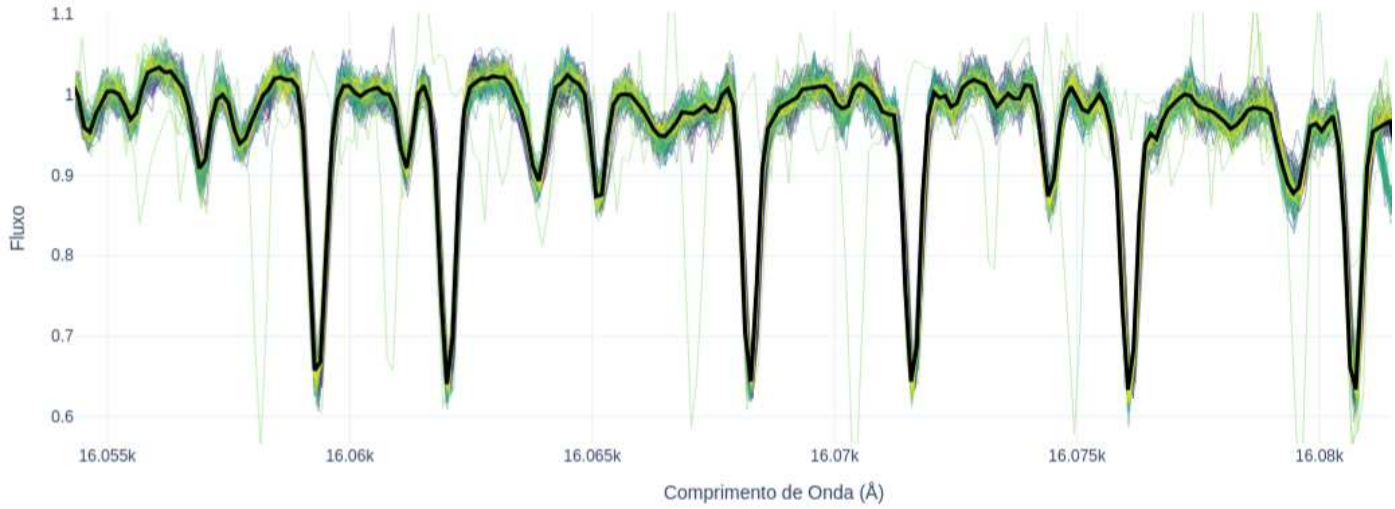

Figure 1. A portion of the combined spectrum of GJ 3470 in the 16055-16080 Å. Black trace: combined spectrum; colored lines: individual observations.

Table 1. Resultados derivados para o sistema GJ 3470 e o planeta GJ 3470 b, utilizando $M_\star = 0.435$ e $R_\star = 0.4604$.

Parameter	Value	Unit	Equivalent
Semi-major axis	0.331 ± 0.0005	AU	–
Insolation ($S/S_\odot$)	33.289 ± 2.516	–	–
Equilibrium temperature ($T_{\rm eq}$)	597.1 ± 12.23	K	–
Mass	11.02 ± 0.65	Earth masses	0.0346 ± 0.0021 Jupiter masses
Radius	4.06 ± 0.09	Earth radii	0.369 ± 0.008 Jupiter radii
Density	0.909 ± 0.082	g cm^{-3}	–
Gravity	6.58 ± 0.49	m s^{-2}	–

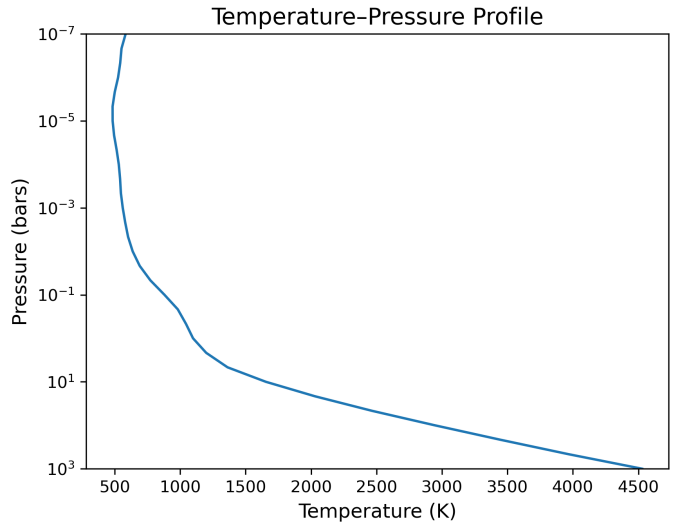

Figure 2. Temperature-pressure profile modeled for the atmosphere of GJ 3470 b using the PICASO code. The curve shows the variation in temperature with pressure throughout the atmospheric column.

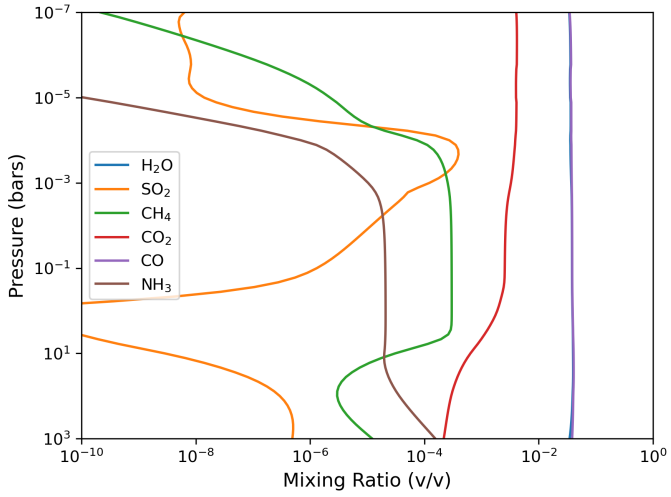

Figure 3. Chemical abundances for H_2O, CO, CO_2, CH_4, NH_3, and SO_2 in the atmosphere of GJ 3470 b as a function of pressure.

with SPIRou and atmospheric modeling of the exoplanet GJ 3470 b. The combined stellar spectrum enabled the determination of the host star's effective temperature and metallicity, providing key inputs for interpreting the planet's atmospheric properties.

Using these stellar parameters, we modeled the atmosphere of GJ 3470 b with JWST/NIRCam data and the `PICASO` code, coupled with Bayesian sampling via MCMC. The results point to an atmosphere with a metallicity roughly 100 times the solar value, a C/O ratio near the upper limit of the explored range (~0.92), and strong vertical mixing, characterized by $\log K_{zz} \approx 9$. The inferred heat-redistribution efficiency (heat$_{\rm r}$edis ≈ 0.4) suggests substantial transport of energy to the nightside. In contrast, the cloud-settling parameter ($f_{\rm sed} \approx 3$) indicates the presence of

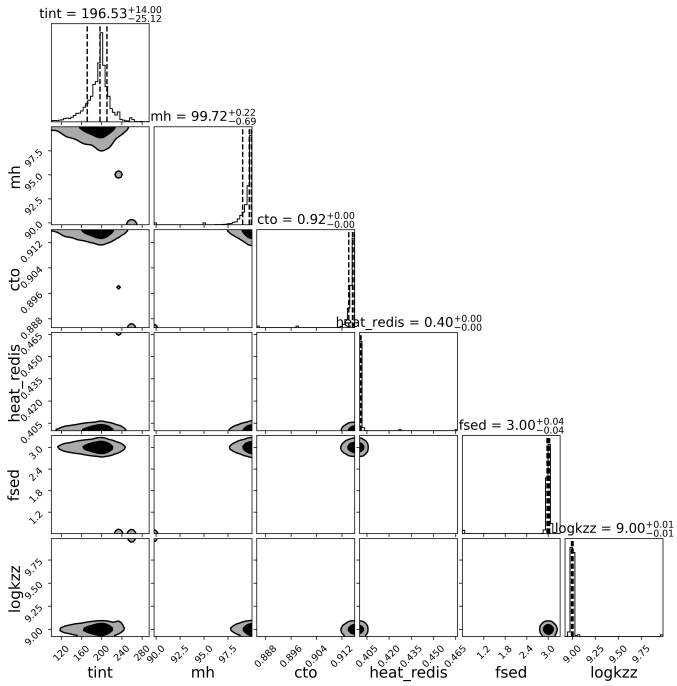

Figure 4. Subsequent distributions of atmospheric parameters inferred for GJ 3470 b.

moderately thick clouds. We also identified signatures of SO_2, CO_2, and H_2O. Collectively, these results reveal that GJ 3470 b hosts a dynamic, metal-enriched atmosphere shaped by both vertical transport and photochemical processes.

Acknowledgements. CC, DS, and ASA acknowledge support from the Foundation for Research and Technological Innovation Support of the State of Sergipe (FAPITEC/SE) and the National Council for Scientific and Technological Development (CNPq), under grant numbers 404056/2021-0, 794017/2013, and 444372/2024-5.

References

Batalha, N. M., Rowe, J. F., Bryson, S. T., et al. 2013, *ApJS*, 204, 24
Batalha, N. E., Marley, M. S., Lewis, N. K., & Fortney, J. J. 2019, *ApJ*, 878, 70
Beatty, T. G., Welbanks, L., Schlawin, E., et al. 2024, *ApJL*, 970, L10
Bean, J. L., Raymond, S. N., & Owen, J. E. 2021, *JGR: Planets*, 126, e2020JE006639
Blanton, M. R., Bershady, M. A., Abolfathi, B., et al. 2017, *AJ*, 154, 28
Borucki, W. J., Koch, D., Basri, G., et al. 2010, *Science*, 327, 977
Cook, N. J., Artigau, É., Doyon, R., et al. 2022, *PASP*, 134, 114509
Donati, J. F., Kouach, D., Moutou, C., et al. 2020, *MNRAS*, 498, 5684
Melo, E., Souto, D., Cunha, K., et al. 2024, *ApJ*, 973, 90
Wanderley, F., Cunha, K., Smith, V. V., et al. 2025, *ApJ*, 993, 233
Foreman-Mackey, D., Hogg, D. W., Lang, D., & Goodman, J. 2013, *PASP*, 125, 306
Gustafsson, B., Edvardsson, B., Eriksson, K., et al. 2008, *A&A*, 486, 951
Henry, T. J., Jao, W.-C., Subasavage, J. P., et al. 2006, *AJ*, 132, 2360
Mann, A. W., Feiden, G. A., Gaidos, E., et al. 2015, *ApJ*, 804, 64
Masseron, T., Merle, T., & Hawkins, K. 2016, *ASCL*, ascl:1605.004
Mukherjee, S., Batalha, N. E., Fortney, J. J., & Marley, M. S. 2023, *ApJ*, 942, 71
Petigura, E. A., Howard, A. W., & Marcy, G. W. 2013, *PNAS*, 110, 19273
Plez, B. 2012, *ASCL*, ascl:1205.004
Ricker, G. R., Latham, D. W., Vanderspek, R. K., et al. 2010, *AAS Meeting Abstracts*, 215, 450.06
Rooney, C. M., Batalha, N. E., Gao, P., & Marley, M. S. 2022, *ApJ*, 925, 33
Souto, D., Cunha, K., Smith, V. V., et al. 2020, *ApJ*, 890, 133